Dissolution and Reprecipitation Behavior of TiC-TiN-Ni Cermets During Liquid-Phase Sintering

Chul Soo Yoon, Shinhoo Kang, and Doh-Yeon Kim

Dept. of Inorganic Materials Eng. Seoul National Univ., Seoul 151-742 Korea
(Received April 20, 1997)

An attempt was made to understand the dissolution and reprecipitation behavior of the constituent phases such as TiC, TiN, and Ti(CN) in TiC-TiN-Ni system. During the liquid-phase sintering the TiC phase was found to dissolve preferentially in Ni binder. The solid-solution phase, Ti(CN), formed around the TiN phase, resulting in a core/rim structure. This result was reproduced when large TiC particles were used with fine TiN particles. The path for the microstructural change in TiC-TiN-Ni system was largely controlled by the difference in the interfacial energy of each phase with the liquid binder phase. The results were discussed with thermodynamic principles.

Key words : Cermets, TiC, TiN, Dissolution, Reprecipitation, Surface energy

I. Introduction

TiC-based cermets was introduced along with Ni binder as a potential candidate material for cutting tool applications. The TiC phase provides excellent properties such as high hardness, low specific density, and high-temperature chemical stability. However, its inherent low toughness and poor compatibility (wettability) with liquid Ni have become its limitation for broader uses. A refreshed attention was made as the additions of various transitional metal carbides and nitrides improved the critical properties.[1-3] In particular, the addition of nitrogen to TiC significantly improved the toughness, thermal shock resistance and chemical stability of the TiC-Ni based cermets.[4-6] Nitrogen has been added by nitriding TiC powder or by ball-milling TiC with TiN. It was reported that the nitrogen addition inhibited grain growth when the 1:1 ratio of C to N and TiN was used up to 15 wt. % in Ti(CN)-Ni and TiC-TiN-Ni systems, respectively.[7,8] Also, the control of nitrogen partial pressure during heating and sintering process became an important parameter to improve the mechanical properties of cermets.[9,10] Assisted with recent developments in this field, Ti(CN)-Ni and TiC-TiN-Ni have been known as common base compositions for commercial cermets.

The mechanism of grain refinement in TiN-containing cermets has not been fully understood yet. A previous work[5] suggested that the formation of a core/rim structure proceeded through the spinodal decomposition of initially formed solid solution. However, a majority of subsequent research works asserted that the rim structure was formed directly during sintering via dissolution and reprecipitation. The complexity in the compositions and processing variables kept the researchers from a thorough understanding in the microstructural development of TiC-TiN-based system. In this paper, the microstructural development of TiC-TiN-Ni system was investigated. Especially the formation sequence of a core/rim structure in hard phases was studied in some details. The results were discussed in terms of the solubility differential of TiC and TiN in nickel binder and total free energy changes of the system.

II. Experimental

TiC and TiN powders obtained from H. C. Starck, Germany and Kennametal, USA, respectively, were used to prepare TiC-TiN-Ni cermets. TiC powders of two different sizes, $TiC_{0.94}$ of 1.69 μm and $TiC_{0.98}$ of 14.5 μm, were selected to examine the size effect on the particle growth during sintering. The average size of $TiN_{0.91}$ was 1.5 μm. Two compositions, 40%TiC (1.69 μm)-40%TiN-20%Ni and 35%TiC (14.5 μm)-35%TiN-30%Ni (all in wt.%), were prepared for this study. An infiltration technique was used to produce sandwiched specimens consisting of TiC and TiN layers as shown in Fig. 1. This was to understand the dissolution behavior and material transfer between TiC and TiN particles.

The TiC and TiN powders were slurry-mixed using ethanol as a solvent. The skeletons for the infiltration were prepared by compacting the powders under 100 MPa pressure. Nickel infiltrants were made using the same conditions and placed on the skeletons prior to heating. The specimens were heated at 10°C/min with a hold at 500°C for 0.5 hr. The infiltration was completed at 1450°C in vacuum, using a graphite furnace. Sintering time and vacuum level were 0.5~2 hours and 17.3 Pa, respectively. X-ray diffraction analysis, optical and scan-
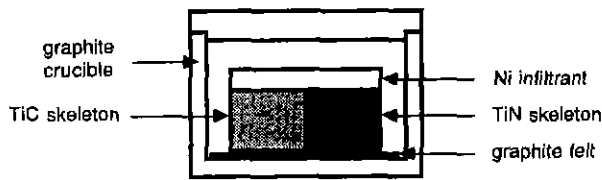
Fig. 1. Schematic illustration of the sandwiched specimen.

ning electron microscopy were performed to study the microstructure of the cermets.

III. Results and Discussion

1. Effect of TiN on the Dissolution of TiC

The TiC and TiN phases of B1 (NaCl) structure are known to form the Ti(CN) phase with ease when those are reacted together at relatively high temperatures. Figure 2 shows the microstructure of 40%TiC (1.69 μm)-40% TiN-20%Ni cermets. The sample was sintered at 1450°C for 0.5 hr. The hard phase surrounded by white-colored Ni binder phase often exhibits a core/rim structure. Optical microscopy revealed that all the cores were distinctive TiN particles in a golden color while the rim consisted of a gray Ti(CN) solid solution. The formation of Ti(CN) prevailed in TiC-TiN-Ni system and the microstructure was expected to move toward a homogeneous Ti(CN)-Ni. From this observation it seemed that a preferential dissolution of the TiC phase had occurred extensively during sintering.

Sandwiched specimens were prepared by placing the same amount of TiC and TiN powders as shown in Fig. 1. It was to study the progress in microstructural changes during liquid-phase sintering. A special attention was paid on the microstructural changes in the region of TiC/TiN boundary. Figure 3 shows typical SEM micrographs of each region: (a) a central region of the TiC layer, (b) a boundary region in the TiC layer near the TiC/TiN interface, (c) a boundary region in the TiN layer near the TiC/TiN interface, and (d) a central region of the TiN layer.
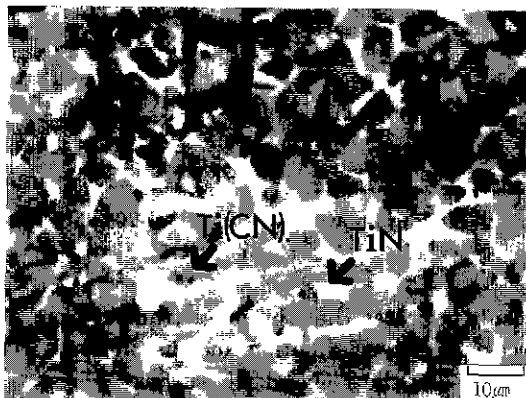

Fig. 2. The microstructure of 40%TiC-40%TiN-20% Ni specimen sintered at 1450°C for 0.5 hr in vacuum.

Comparing Fig. 3(a) and 3(b), the particle size of TiC in Fig. 3(b) is significantly smaller than that in Fig. 3(a). But the particle morphology looks the same. Meanwhile, Fig. 3(c) and 3(d) clearly shows a rim structure of Ti(CN) solid-solution layer formed around TiN cores. The thickness of the rim structure of TiN decreased in Fig. 3(d) as the distance increased away from the TiC/TiN boundary. It was found that the shape of those particles in the TiN layer was more faceted than that in the TiC layer. The rounding of TiC particles in the TiC layer means that more or less anisotropic surface energy exists between the liquid and TiC phase in the presence of nitrogen.

The co-existence of TiC and TiN particles as neighboring phases in liquid Ni binder exerted a strong influence on the dissolution behavior of each phase. The TiC particles at the TiC/TiN boundary remained considerably small compared to TiN. However, the overall size of the TiC particles in Fig. 3(b) increased to 2~5 μm from their original particle size (1~2 μm). Also, the TiN cores in Fig. 3(c) and 3(d) grew noticeably (3~10 μm) compared to the initial TiN particles (1.5 μm). Figure 3 suggests the following possibilities during the sintering process, i.e., (1) the presence of TiN with TiC enhances the preferential dissolution of TiC and/or (2) the presence of TiN tends to slow the coarsening of TiC. It is not plausible that the majority of the core-coarsening was achieved through the decomposition of Ti(CN) at the core/rim interface. Thus, the increase in the particle size of TiC and TiN cores could be explained by the coalescence during the initial stage of sintering.[1,2] With this reasoning the first possibility seems to be dominant.

An additional experiment was done to confirm the dissolution behavior of TiC in TiN environment. The cermets of TiC-30%Ni and TiC-35%TiN-30%Ni (in wt.%) were prepared in the same way using coarse TiC powder (14.5 μm). The coarse TiC powder reduces the TiC surface energy per unit volume. Thus, a reverse development, i.e., TiC particle growth along with TiN dissolution, would happen if the observed dissolution of TiC was related only to the particle size and to the minor difference in surface energy between TiC and TiN in liquid Ni. However, as shown in Fig. 4, the coarse TiC particles in TiC-35%TiN-30%Ni dissolved completely and reprecipitated around TiN. The TiC particles in TiC-30% Ni on the other hand, grew exceeding the original particle size in the matrix. This confirms that the size of TiC has little influence in determining the microstructure of the TiC-TiN-Ni mixture and the difference in the surface energy between TiC and TiN is remarkable.

Figure 5 shows the microstructures of another specimens sintered 1450°C for 0.5 and 2 hours, respectively. The specimen has a TiC layer placed between two TiN layers. It demonstrated that the width of the TiC layer decreased as the sintering time was lengthened. This example demonstrates again that the dissolution of TiC
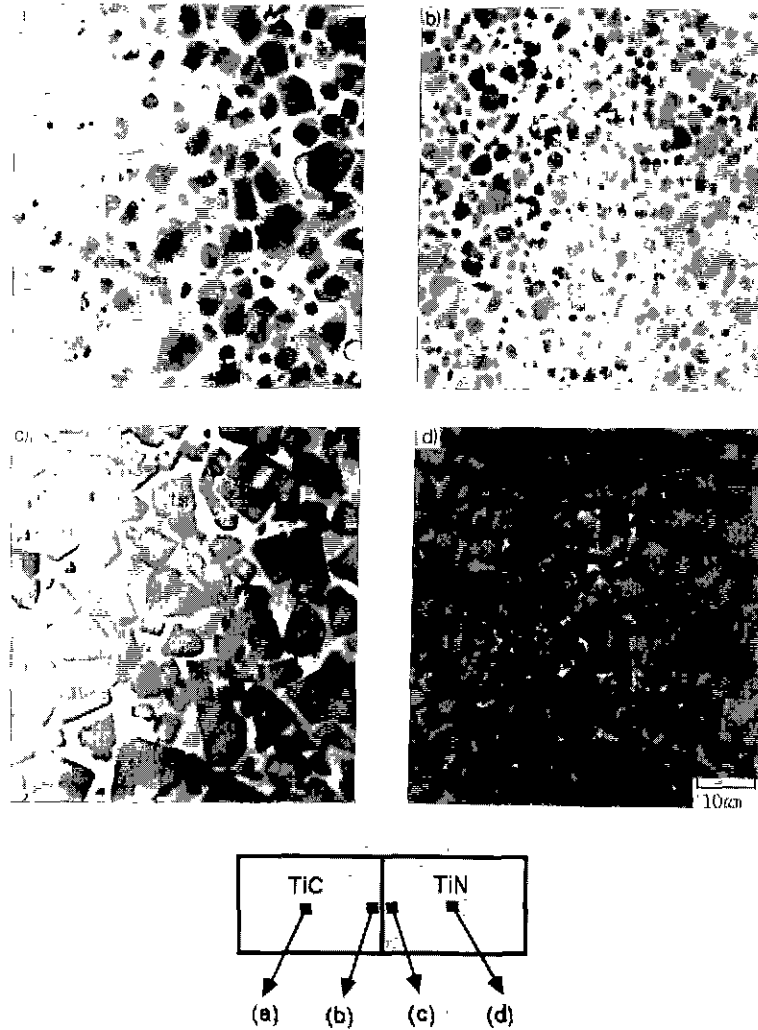
Fig. 3. The microstructure of the sandwiched specimen sintered at 1450°C for 0.5 hr in vacuum. a) Center of the TiC layer, b) Interface region of the TiC layer, c) Interface region of the TiN layer, d) Center of the TiN layer.
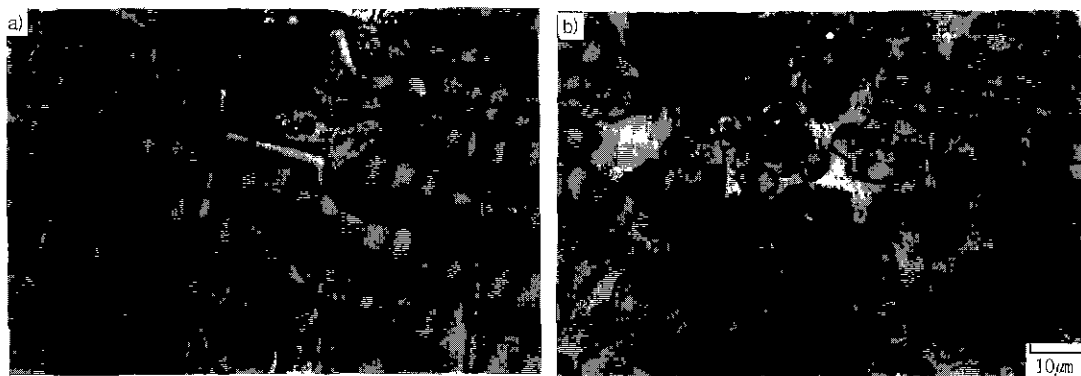
Fig. 4. Microstructure of the specimen sintered at 1450°C for 0.5 hr in vacuum (14.5 μm powder was used). a) 70%TiC-30%Ni, b) 35%TiC-35%TiN-30%Ni.

was dominant over the inhibiting effect of TiN on the growth of TiC. Further, the particles in the TiC layer were found to be Ti(CN) proven by a slow etching response. These particles were contrasted with the remaining TiC particles at the boundary region in Fig. 3(b).

This result indicates that the mass transfer from TiC to TiN occurred as the formation and dissolution of Ti(CN) were repeated at the TiC and TiN surfaces.

An X-ray diffraction analysis was done to understand the extent of solid-state reaction among TiC and TiN par-
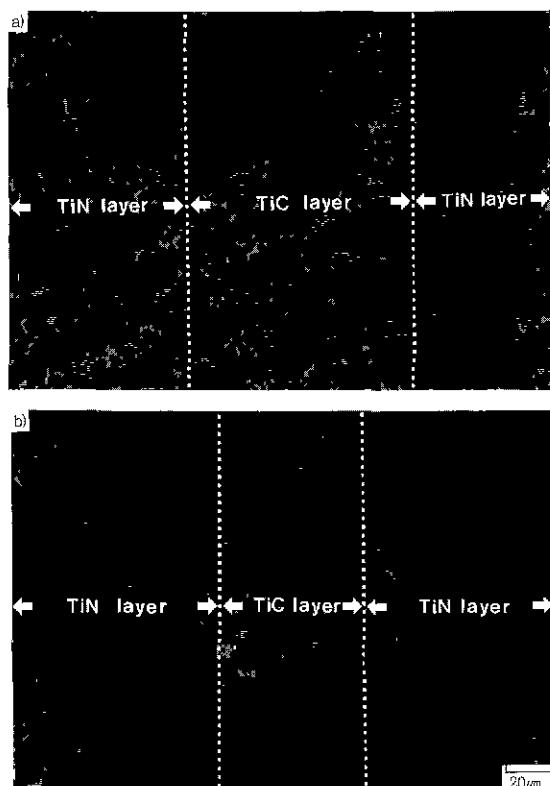
Fig. 5. The microstructure of the sandwiched specimen sintered at 1450°C. a) for 0.5 hr, b) for 2 hr.

Fig. 6. X-ray diffraction patterns of the specimens heat treated at 1300°C for 0 hr. a) TiC, b) TiN, c) TiC+TiN.

ticles prior to liquid-phase sintering. The specimens were heated to various temperature and immediately cooled down to room temperature. Ni infiltrant was often observed to melt near 1300°C, lower than its intrinsic melting temperature (1453°C), due to carbon diffusion. The analysis for the skeleton, as shown in Fig. 6, showed only TiC and TiN peaks. This indicated that there was a minor solid-state reaction to form Ti(CN) up to 1300°C. Since it is known that TiC has a higher tendency to coarsen than TiN at the initial stage of sintering11, the preferential dissolution of TiC in the presence of TiN and subsequent Ti(CN) formation are evident.

2. Reprecipitation of Ti(CN) on TiN Cores

In general, the coarsening of single-phase particles dispersed in a liquid phase is due to the curvature effect known as Thompson-Freundlich relationship.[12] A massive material transfer from TiC to TiN in this study could be explained with this relationship to a certain extent. The Ti solubilities in liquid Ni of TiC-Ni and TiN-Ni were reported to be 7 and 5 wt.%, respectively.[7] If the equilibrium solubility is assumed to be 7 wt.%, the calculated difference in the solubility by the curvature effect is limited to a few hundredths of a percentage for commercial powder sizes.[13] It means that the equilibrium solubilities of TiC and TiN in the binder played a major role in coarsening for these mixture system. In the present case the growth of the hard phase, Ti(CN), in-
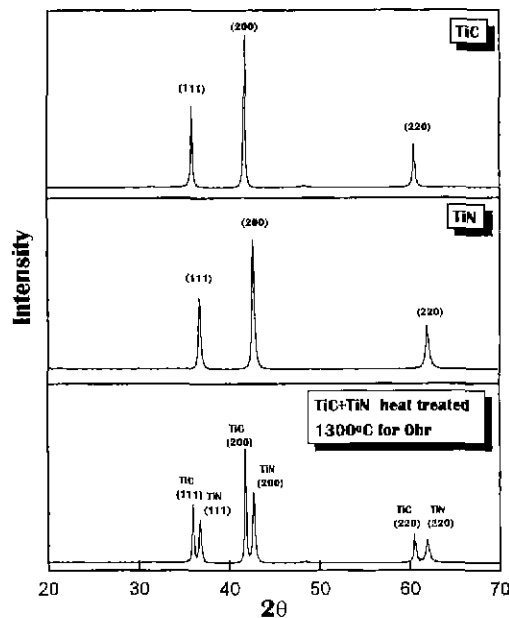
volves two phases of different interfacial energy. The common factors controlling the microstructural changes in a system are free energy changes associated with new phase formations, surface energy and interfacial strain.

The formation of a solid solution is generally favored due to the entropy of mixing unless repulsion exists among the constituents in the mixture. From the experimental results the formation of Ti(CN) by the mixing of TiC and TiN showed a strong negative deviation from ideal mixing.[14-16] Thus, this factor is expected to be the major driving force in microstructural changes. Also, the reprecipitation of Ti(CN) on the cores entails a small lattice mismatch. This raises the free energy due to the strain factor. The changes in the surface free energy are associated with various contributors. The reduction in TiC/Ni and TiN/Ni surface area will decrease free energy related to the surfaces. Whereas the generation of new Ti(CN)/Ni and core/rim interfaces will cause the surface energy to increase.

The measurement of wetting angles on a substrate with a liquid metal often provides a useful insight on the surface energy. The wetting angles measured with liquid Ni on TiC and TiN in vacuum are known to be 13° and 115°C respectively.[17] Thus, the TiN/Ni interface which has a higher surface energy than TiC/Ni was expected to disappear to lower the total free energy. This was not achieved by the dissolution of TiN. Rather, as noted from Fig. 2, the TiN/Ni interface was removed by the formation of the Ti(CN) layer around TiN cores along with TiC dissolution.

In the system of current study it could be assumed for Ti(CN) to precipitate at different location, i.e., TiC or TiN surface. The lattice parameters of TiC and TiN are

4.328 and 4.240 A, respectively. It is known that the lattice parameters for various Ti(CN) follows Vegard s law.[18] If Ti($C_{0.5}N_{0.5}$) is to form, the changes in the surface and strain terms induced by Ti(CN)/TiN or by Ti(CN)/TiC interface are about the same. Comparing the changes in total free energy of these two cases, the changes in free energy caused by the formation of Ti(CN) and interfacial stain are almost equivalent each other.

The solubility of nitrogen in Ni at 1450~1500°C is 0.025 at. % while carbon dissolves in Ni up to 9% in the temperature range. The low solubility of nitrogen in Ni could result in a higher carbon content in Ti(CN) than 0.5. Then, the Ti(CN) will have a better match with TiC than with TiN. This makes the strain energy term for the Ti(CN)/TiN more positive than that of Ti(CN)/TiC. Taking this fact into consideration, the difference in the surface energies of TiC-Ni and TiN-Ni interfaces is large enough to compensate the effect of the strain energy difference. Therefore, it was the surface energy that determines the microstructure change from the initial TiC-TiN-Ni system.

IV. Summary and Conclusions

The microstructure of TiC-TiN-Ni system was studied to understand the dissolution and reprecipitation behavior during liquid phase sintering. TiC and TiN of a similar particle size and equi-weight percent were used with Ni in this experiment. During the sintering the TiC particles tended to dissolve preferentially over the TiN phase in liquid Ni. This was reproduced with a system of significantly large TiC particles (14.9 μm). Also, the Ti (CN) phase always formed around the TiN particles, exhibiting a core/rim structure. It was concluded from this study that the driving force for the development of the TiC-TiN-Ni microstructure resulted from the free energy reduction by the Ti(CN) formation and the removal of TiN/Ni high energy surface area.

Acknowledgment

References

1. M. Humenik JR. and Niranjan M. Parikh, *J. Am. Ceram. Soc.*, **39**[2], 60-63 (1956).
2. N. M. Parikh and M. Humenik, JR. *J. Am. Ceram. Soc.*, **40**[9], 315-320 (1957).
3. Ohtsuki E., Fujita H. and Masuda V., *Trans. JIM*, **47**, 567 (1983).
4. Nishgaki K., Doi H., Shingyoji T. and Oosawa Y., *J. Japan Soc. of Powder and powd. Met.*, **27**, 160-165 (1980).
5. Rudy E., *J Less-Common Metals*, **33**, 43-70 (1973).
6. Rudy E., Worcester S. and Elkington W., 8th Plansee Seminar II No. 30 (1974).
7. M. Fukuhara and H. Mitani, *Powder Metallurgy*, **25**[2], 62-68 (1982).
8. Nishgaki K. and Doi H., *Japan Soc. of Powder and powd. Met*, **27**, 130-136 (1980).
9. H. Suzuki, K. Hayashi, T. Yamamoto and W. J. Lee *J. Jap. Soc. of Powder and Powd. Met.*, **23**, 224 (1976).
10. H. Suzuki, K. Hayashi, Y. Kubo and H. Matsubara, *J. Jap. Soc. of Powder and Powd. Met.*, **28**, 147 (1981).
11. M. Fukuhara and H. Mitani, *Powder Met. International*, **14**[4], 196-200 (1982).
12 G. W. Greenwood, *Acta Met.*, **4**, 243-248 (1956).
13. C. S. Yoon, M.S. Thesis, Seoul National Univ., Seoul, (1995).
14. R. Kieffer, P. Ettmayer, and M. Freundhofmeier, *Modern Development in P/M*, **5**, 201 (1971).
15. H. L. Schick, Thermodynamics of Certain Refractory Compounds, Vol I and II, Academy Press, New York, 1966.
16. A. N. Zelikman and N. N. Gorowitz, *J. Pril. Khim.*, **23**, 689 (1950).
17. G. A. Yasinskaya, *Poroshkovaya Metallurgiya*, **7**[43], 55-56 (1965).
18. H. Pastor, *Mat. Sci. Eng.*, **A105/106**, 410 (1988).